

Thermal Expansion of Simulated Spent PWR Fuel and Simulated DUPIC Fuel¹

K. H. Kang,^{2,3} K. C. Song,² and M. S. Yang²

Thermal expansions of simulated spent PWR fuel and simulated DUPIC fuel were studied using a dilatometer in the temperature range from 298 to 1900 K. The densities of simulated spent PWR fuel and simulated DUPIC fuel used in the measurement were $10.28 \text{ g} \cdot \text{cm}^{-3}$ (95.4% of TD) and $10.26 \text{ g} \cdot \text{cm}^{-3}$ (95.1% of TD), respectively. The linear thermal expansions of the simulated fuels are higher than that of UO_2 , and the difference between these fuels and UO_2 increases progressively with temperature. However, the difference between simulated spent PWR fuel and simulated DUPIC fuel is extremely small, less than the experimental error. For the temperature range from 298 to 1900 K, simulated spent PWR fuel and simulated DUPIC fuel have the same average linear thermal expansion coefficient of $1.39 \times 10^{-5} \text{ K}^{-1}$. As the temperature increases to 1900 K, the relative densities of simulated spent PWR fuel and simulated DUPIC fuel decrease to 93.8% of initial densities at 298 K.

KEY WORDS: density; simulated DUPIC fuel; simulated spent PWR fuel; thermal expansion.

1. INTRODUCTION

The concept of the direct use of spent PWR fuel in CANDU reactors (DUPIC) is a dry processing technology to manufacture CANDU fuel from spent PWR fuel material without separating fissile materials and fission products in the fuel. Spent PWR fuel typically contains 0.9 wt%

¹ Paper presented at the Sixteenth European Conference on Thermophysical Properties, September 1–4, 2002, London, United Kingdom.

² Korea Atomic Energy Research Institute, P.O. Box 105, Yusong, Taejeon 305-600, South Korea.

³ To whom correspondence should be addressed. E-mail: nghkang@kaeri.re.kr

fissile uranium and 0.6 wt% fissile plutonium, which exceeds the natural uranium fissile content of 0.71 wt%. The neutron economy of a CANDU reactor is sufficient to allow DUPIC fuel to be used in a CANDU reactor, which is originally designed for natural uranium fuel. The concept was proposed and termed DUPIC fuel cycle by the Korea Atomic Energy Research Institute (KAERI) and Atomic Energy Canada Limited (AECL) in participation with U.S.A. in 1991 [1, 2]. The DUPIC fuel cycle offers several benefits to countries with both PWR and CANDU reactors: no need for spent PWR fuel disposal, saving natural uranium resources for the fabrication of CANDU fuel, and extended burnup of CANDU fuel by utilizing the DUPIC fuel.

The main characteristic of DUPIC fuel is its initial content of fission products as impurities. The thermal properties of DUPIC fuel are expected to be different from CANDU fuel because of the fission products. The thermal properties of this fuel material should be known to assess the behavior of fuel elements at high temperature in reactors. The thermal expansion of nuclear fuel is one of the most important properties because it affects the gap conductance and interaction with cladding. It also causes the density variation with temperature, which is used for calculation of other properties such as thermal conductivity.

The importance of the thermal expansion of nuclear fuel has led to numerous experimental studies using high temperature X-ray and neutron diffraction techniques [3–10] and the dilatometer [11, 12]. X-ray and neutron diffraction provide lattice parameters, and the dilatometer provides macroscopic length changes including the effects of the Schottky defect. Gronvold [3], Baldock et al. [4], and Albinati et al. [5] measured the lattice parameters of uranium oxides with temperature and found the coefficients of linear thermal expansion. Hutchings [6] and Tyagi and Mathews [10] investigated the thermal expansions by measuring the lattice parameters with temperature of $(\text{Th}, \text{U})\text{O}_2$. Momin et al. [7] studied the lattice thermal expansion behavior of UO_2 , ThO_2 , and $(\text{U}_{0.2}\text{Th}_{0.8})\text{O}_2$ doped with fission product oxides. Yamishita et al. studied the thermal expansions of NpO_2 and some other actinide dioxides [8] and $(\text{Np}, \text{U})\text{O}_2$ [9]. Tokar et al. [11] and Lorenzelli and El Sayed Ali [12] measured the thermal expansion of PuO_2 and $(\text{U}, \text{Pu})\text{O}_{2-x}$, respectively, using a dilatometer. Martin [13] reviewed the available expansion data related to UO_2 and (U, Pu) mixed oxides and recommended fitting equations and coefficients of the thermal expansion of these materials.

In the case of DUPIC fuel, the direct measurement of the thermal properties is very difficult in a laboratory due to its high level of radioactivity. As a part of a DUPIC fuel development program, the thermal properties have been investigated using simulated DUPIC fuel. Simulated fuels

(simulated spent PWR fuel and simulated DUPIC fuel) provide a convenient way to investigate the intrinsic fuel thermal properties.

In this study the thermal expansions of simulated spent PWR fuel and simulated DUPIC fuel are measured using the dilatometer in the temperature range of 298 to 1900 K to estimate the thermal expansion and density variation with temperature of DUPIC fuel.

2. EXPERIMENTAL

2.1. Sample Preparation and Characterization

Simulated reference DUPIC fuel was used in this study. The DUPIC fuel composition, as the reference, was proposed by neutronic calculation such that the enrichment levels of U-235 and Pu-239 are 1.0 and 0.45 wt%, respectively. Simulated spent PWR fuel was fabricated by compaction and sintering the powder prepared by adding stable oxides as surrogates for fission products to UO_2 . Simulated DUPIC fuel pellets were fabricated by compaction and sintering of the powder prepared through the OREOX (oxidation and reduction of oxide fuel) process of simulated spent PWR fuel. The fission product composition of irradiated fuel was determined by its initial enrichment and irradiation history. The ORIGEN (Oak Ridge Isotope Generation and Depletion) code was used to calculate the compositions of fission products, which were added into UO_2 powder. The fourteen elements listed in Table I represent the major fission products except for volatile elements.

To prepare simulated spent PWR fuel, the mixed powder of UO_2 and additives was pressed with $3 \text{ ton} \cdot \text{cm}^{-2}$ into green pellets, and sintered at 1973 K for 4 hours in the flowing 100% H_2 gas stream. Simulated DUPIC fuel was fabricated using powder prepared through the OREOX process of

Table I. Contents of Surrogates for Fission Products Added to UO_2 Powder

Fission products	Composition (wt.%)	Fission products	Composition (wt.%)
Zr (ZrO_2)	0.422	Pr (Nd_2O_3) ^a	0.131
Mo (MoO_3)	0.392	Nd (Nd_2O_3)	0.476
Ru (RuO_2)	0.269	Sm (Nd_2O_3) ^a	0.101
Pd (PdO)	0.187	Sr (SrO)	0.084
Ba (BaCO_3)	0.218	Y (Y_2O_3)	0.052
La (La_2O_3)	0.143	Rh (Rh_2O_3)	0.049
Ce (CeO_2)	0.278	Te (TeO_2)	0.058

^a Pr and Sm were replaced by Nd_2O_3 .

simulated spent PWR fuel in the same procedure as above, i.e., conventional pre-compaction, granulation, pressing with $3 \text{ ton} \cdot \text{cm}^{-2}$, and sintering at 1973 K for 4 hours in the flowing 100% H_2 gas stream. The OREOX process was repeated 3 times with oxidation at 723 K and reduction at 923 K. Complete descriptions of the fabrication methods and characterization results have been provided in a previous publication [14]. The theoretical density of simulated spent fuel proposed Lucuta et al. [15] was used in calculation of relative density of simulated spent PWR fuel and simulated DUPIC fuel. The densities of simulated spent PWR fuel and simulated DUPIC fuel were $10.28 \text{ g} \cdot \text{cm}^{-3}$ (95.4% of TD) and $10.26 \text{ g} \cdot \text{cm}^{-3}$

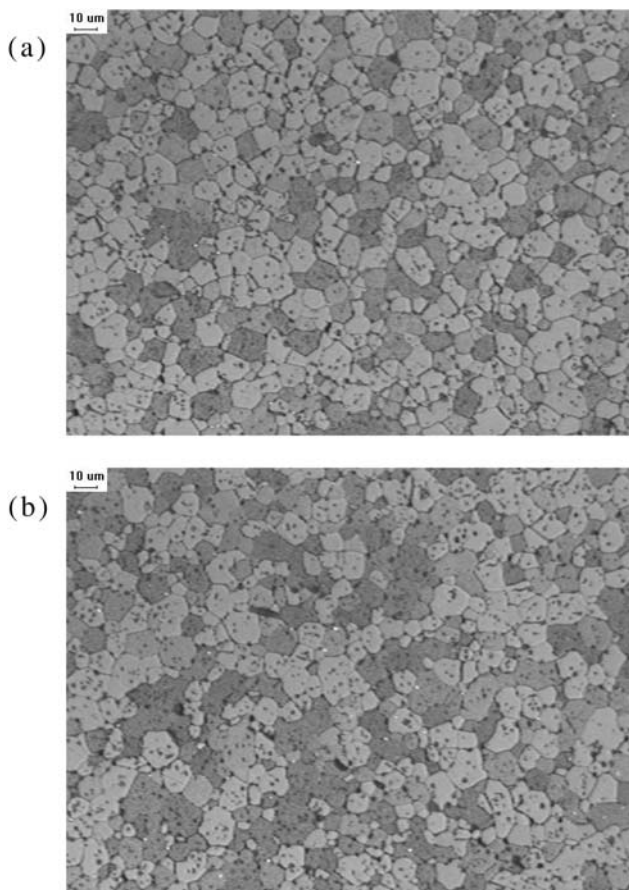


Fig. 1. Optical microscope image of (A) simulated spent PWR fuel and (B) simulated DUPIC fuel ($\times 500$).

(95.1% of TD), respectively. It can be assumed that the specimens used in the experiment are stoichiometric because they are sintered in conditions of 100% H₂ at high temperature. The microstructures of the pellets are shown in Fig. 1. Simulated spent PWR fuel and simulated DUPIC fuel have almost the same microstructure and grain size. The grain size of simulated fuel is 10 μm. The compositions and contents of precipitates in the simulated fuel pellets were investigated using an electron probe micro-analyzer (EPMA) as in our previous study [14]. It was noted that the oxide precipitates contained mainly Zr and Ba, which had a barium zirconate-type perovskite phase. The spherical metallic precipitates, which were distributed in the grain boundaries, contained Mo, Ru, Pd, and Rh. The other additives such as Zr, Y, La, Nd, and Ce were dissolved in the matrix. This result was very similar to that of Lucuta et al. [15].

2.2. Measurement of Thermal Expansion

The thermal expansions of the simulated fuel pellets were measured in the axial direction with a linear variable differential transformer (LVDT) transducer in the temperature range of 298 to 1900 K by a push-rod-type dilatometer (DIL 402 C, Netzsch). The measurements were carried out with a constant heating rate of 5 K·min⁻¹ in vacuum. Maximum error of the dilatometer used in our experiment is within 2% for a standard material of Al₂O₃.

3. RESULTS AND DISCUSSION

The linear thermal expansion which represents the ratio of the length change to the initial length can be calculated using the following expression:

$$\text{Expansion, } \frac{\Delta L}{L_0}, \% = \frac{L_T - L_{298}}{L_{298}} \times 100, \quad (1)$$

where L_T and L_{298} represent the lengths of specimens at temperature T and at 298 K, respectively. The linear thermal expansions of simulated spent PWR fuel, simulated DUPIC fuel, and UO₂ determined in this study are plotted against temperature in Fig. 2. Martin [13] reviewed available data of UO₂ thermal expansions and recommended a third-degree polynomial equation as a function of temperature for representing the linear thermal expansion of UO₂. The combined linear and exponential equation as a function of temperature is used in MATPRO [16]. The computational results from these equations are also shown in Fig. 2 for the purpose of comparison.

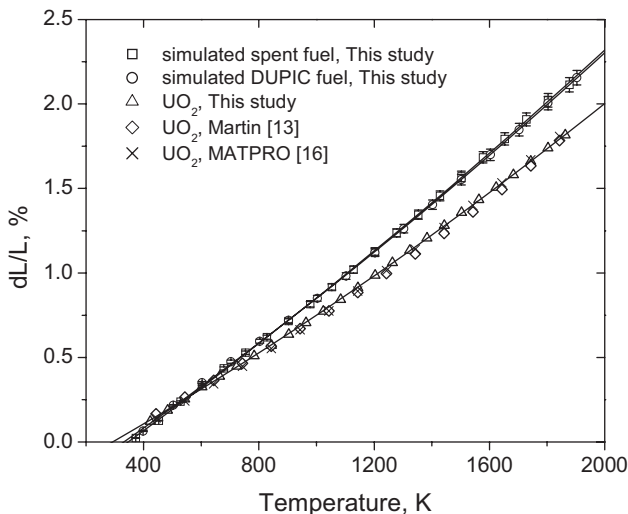


Fig. 2. Linear thermal expansions of simulated spent fuel, simulated DUPIC fuel, and UO_2 as a function of temperature.

From the figure, as expected, it is observed that the linear thermal expansions of all the specimens increase progressively with temperature. The linear thermal expansion of UO_2 obtained in this study is in good agreement with other results. For simulated fuels, it is higher than that of UO_2 , and the difference between these fuels and UO_2 increases progressively with temperature. However, the difference between simulated spent PWR fuel and simulated DUPIC fuel can be hardly observed because the characteristics such as densities, grain sizes, compositions, and contents of these fuels are almost identical. The thermal expansions obtained in this study are fitted by the following equations:

For simulated spent PWR fuel,

$$\Delta L/L_0(\%) = -0.4163 + 1.170 \times 10^{-3}T + 9.881 \times 10^{-8}T^2 \pm 0.0087. \quad (2)$$

For simulated DUPIC fuel,

$$\Delta L/L_0(\%) = -0.3854 + 1.130 \times 10^{-3}T + 1.095 \times 10^{-7}T^2 \pm 0.0089. \quad (3)$$

For UO_2 ,

$$\Delta L/L_0(\%) = -0.2783 + 9.171 \times 10^{-4}T + 1.118 \times 10^{-7}T^2 \pm 0.0015. \quad (4)$$

In the above equations, the last terms represent the standard deviations.

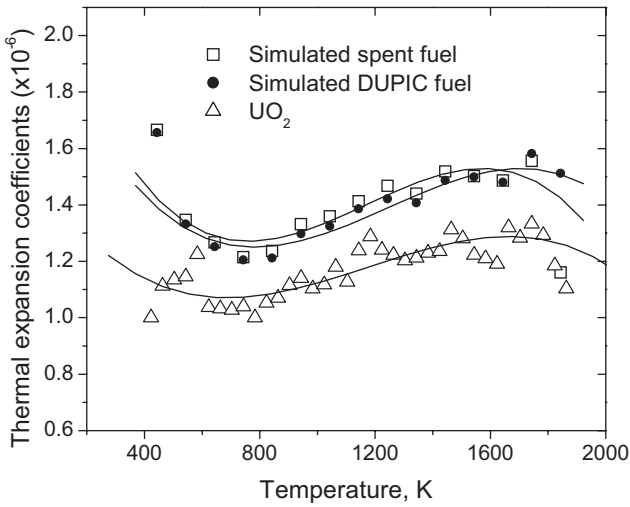


Fig. 3. Instantaneous thermal expansion coefficients of simulated spent PWR fuel, simulated DUPIC fuel, and UO_2 .

The corresponding instantaneous coefficient of thermal expansion, α , is defined by the following expression:

$$\alpha = \frac{1}{L_{298}} \frac{dL}{dT}, \quad (5)$$

The instantaneous thermal expansion coefficients of simulated spent PWR fuel, simulated DUPIC fuel, and UO_2 determined in this study are plotted against temperature in Fig. 3.

From the figure it is observed that the instantaneous thermal expansion coefficients of the simulated fuels are similar to each other and higher than that of UO_2 . The instantaneous coefficient of thermal expansion derived in this study are fitted by the following equations:

For simulated spent PWR fuel,

$$\alpha = 2.39 \times 10^{-5} - 3.49 \times 10^{-8}T + 3.40 \times 10^{-11}T^2 - 9.69 \times 10^{-15}T^3 \pm 5.28 \times 10^{-7}. \quad (6)$$

For simulated DUPIC fuel,

$$\alpha = 2.19 \times 10^{-5} - 2.84 \times 10^{-8}T + 2.65 \times 10^{-11}T^2 - 7.10 \times 10^{-15}T^3 \pm 4.81 \times 10^{-7}. \quad (7)$$

For UO_2 fuel,

$$\alpha = 1.55 \times 10^{-5} + 1.61 \times 10^{-8}T - 1.66 \times 10^{-11}T^2 - 4.70 \times 10^{-15}T^3 \pm 5.25 \times 10^{-7}. \quad (8)$$

In the above equations, the last terms represent the standard deviations.

The coefficient of average linear thermal expansion, $\bar{\alpha}$, is defined by the following equation:

$$\bar{\alpha} = \frac{1}{L_{298}} \times \left(\frac{L_T - L_{298}}{T - 298} \right). \quad (9)$$

For the temperature range from 298 to 1900 K, simulated spent PWR fuel and simulated DUPIC fuel have the same average linear thermal expansion coefficient of $(1.39 \pm 0.12) \times 10^{-5}$, and that of UO_2 is $(1.18 \pm 0.14) \times 10^{-5} \text{ K}^{-1}$. Second terms inside the parentheses represent error bounds. These results are in agreement with those from Momin et al. [8]. He found that coefficients of average linear thermal expansions for UO_2 and the solid solution of UO_2 with 20 wt% Ln_2O_3 ($\text{Ln} = \text{La}, \text{Nd}, \text{Ce}, \text{Y}, \text{Sm}, \text{Gd}, \text{and Eu}$) are 10.8×10^{-6} and $14.3 \times 10^{-6} \text{ K}^{-1}$, respectively. The higher values for the simulated fuels indicate that the partial substitution of U^{+4} with ($\text{Y}, \text{La}, \text{Nd}, \text{and Ce}$)³⁺ added in simulated fuels results in weakening the interatomic bonding in the solid solution matrix.

The density variations with temperature can be obtained from the thermal expansion data using the following equation:

$$\rho(T) = \rho(298) \left(\frac{L_{298}}{L_T} \right)^3, \quad (9)$$

where $\rho(T)$ and $\rho(298)$ represent the densities of specimens at temperature T and at 298 K, respectively.

The relative density ($\rho(T)/\rho(298) \times 100$) variations to the initial density of simulated spent PWR fuel, simulated DUPIC fuel, and UO_2 determined in this study are plotted against temperature in Fig. 4. Martin [13] and Fink [17] recommended the equations for the density variation of UO_2 . The computational results acquired from these equations are also shown in Fig. 4.

From the figure it is observed that the relative density variations of all the specimens decrease progressively with temperature as expected. For UO_2 , as the temperature increases to 1900 K, the relative density decreases to 94.6% of the initial density at 298 K. The relative density of UO_2 obtained in this study appears slightly lower than the result of Fink [17] except for the low and high temperature ranges. Maximum deviation is

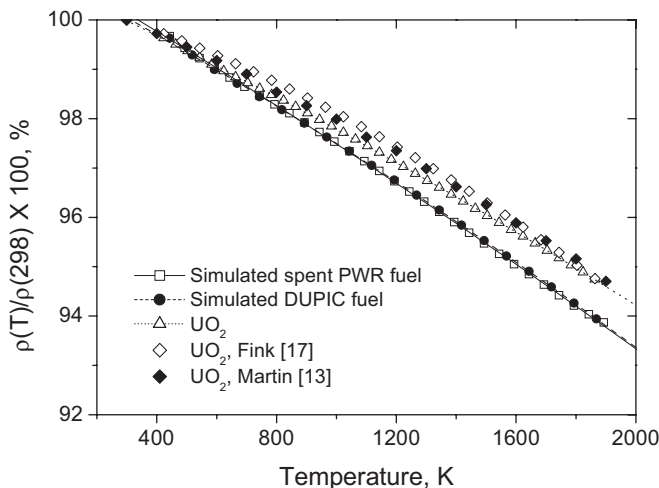


Fig. 4. Density variations of simulated spent fuel, simulated DUPIC fuel, and UO_2 .

2.37% at 950 K. For the simulated fuels, the relative densities are very similar to each other and lower than that of UO_2 . At low temperature to 600 K, the difference of the relative densities of the simulated fuels and UO_2 is small and increases with temperature. As the temperature increases to 1900 K, the relative densities of the simulated fuels decrease to 93.8% of the initial densities at 298 K. The relative densities of simulated spent PWR fuel and simulated DUPIC fuel decrease by 0.78 and 0.83% from that of UO_2 , respectively. The relative density variations with temperature calculated using Eq. (10) are fitted by the following equations:

For simulated spent PWR fuel,

$$\rho(T)/\rho(298) \times 100, \quad \% = 101.206 - 0.0035T - 2.162 \times 10^{-7}T^2 \pm 0.023. \quad (11)$$

For simulated DUPIC fuel,

$$\rho(T)/\rho(298) \times 100, \quad \% = 101.055 - 0.0033T - 2.877 \times 10^{-7}T^2 \pm 0.015. \quad (12)$$

For UO_2 fuel,

$$\rho(T)/\rho(298) \times 100, \quad \% = 100.855 - 0.0028T - 2.439 \times 10^{-7}T^2 \pm 0.012. \quad (13)$$

In the above equations, the last terms represent the standard deviations.

4. CONCLUSIONS

The thermal expansions of simulated spent fuel and simulated DUPIC fuel were measured using the dilatometer in the temperature range of 298 to 1900 K to estimate the thermal expansion and density variation with temperature of DUPIC fuel, and the following results were obtained.

- (1) The thermal expansions of the simulated fuels are higher than that of UO_2 .
- (2) For the temperature range of 298 to 1900 K, simulated spent PWR fuel and simulated DUPIC fuel have the same average linear thermal expansion coefficient of $(1.39 \pm 0.12) \times 10^{-5} \text{ K}^{-1}$.
- (3) The relative densities of the simulated fuels are lower than that of UO_2 .
- (4) The thermal expansions, the average linear thermal expansion coefficients and density variations of simulated spent PWR fuel and simulated DUPIC fuel are similar to each other.
- (5) The data measured and calculated in this study will be useful for the performance evaluation of in-reactor DUPIC fuel behavior.

ACKNOWLEDGMENT

This work was performed under the Long and Mid-Term Nuclear R&D program sponsored by the Ministry of Science and Technology.

REFERENCES

1. I. J. Hastings, P. G. Boczar, C. J. Allan, and M. Gacesa, *Proc. Sixth KAIF/KNS Annual Conf.*, Seoul, Korea (1991).
2. J. S. Lee, K. C. Song, M. S. Yang, K. S. Chun, B. W. Rhee, J. S. Hong, H. S. Park, and C. S. Rim, *Proc. Int. Conf. on Future Nuclear Systems: Emerging Fuel Cycles and Waste Disposal Options Global '93*, Seattle, Washington (1993).
3. F. Gronvold, *J. Inorg. Nucl. Chem.* **1**:357 (1955).
4. P. J. Baldock, W. E. Spindler, and T. W. Baker, *J. Nucl. Mater.* **18**:305 (1966).
5. A. Albinati, *Acta Cryst. A* **36**:265 (1980).
6. M. T. Hutchings, *J. Chem. Soc., Faraday Trans. 2* **83**:1083 (1987).
7. A. C. Momim, E. B. Mirza, and M. D. Mathews, *J. Nucl. Mater.* **185**:308 (1991).
8. T. Yamashita, N. Nitani, T. Tsuji, and H. Inagaki, *J. Nucl. Mater.* **245**:72 (1997).
9. T. Yamashita, N. Nitani, T. Tsuji, and T. Kato, *J. Nucl. Mater.* **247**:90 (1997).
10. A. K. Tyagi and M. D. Mathews, *J. Nucl. Mater.* **278**:123 (2000).
11. M. Tokar, A. W. Nutt, and T. K. Keenan, *Nuclear Tech.* **17**:147 (1973).
12. R. Lorenzelli and M. El Sayed Ali, *J. Nucl. Mater.* **68**:100 (1977).
13. D. G. Martin, *J. Nucl. Mater.* **152**:94 (1988).

14. K. H. Kang, K. C. Song, J. S. Moon, H. S. Park, and M. S. Yang, *Metals and Materials* **6**:583 (2000).
15. P. G. Lucuta, R. A. Verrall, H. J. Matzke, and B. J. Palmer, *J. Nucl. Mater.* **178**:48 (1991).
16. MATPRO—*A Handbook of Materials Properties for Use in the Analysis of Light Water Reactor Fuel Rod Behaviour*, TREE-NUREG-1005, EG&G Idaho, Inc., Idaho Falls, Idaho.
17. J. K. Fink, *J. Nucl. Mater.* **279**:1 (2000).